Deciphering Electron Interplay at the Fullerene/Sputtered TiO_x Interface: A Barrier-Free Electron Extraction for Organic Solar Cells

Dylan Amelot, Mehrad Ahmadpour, Quim Ros, Hervé Cruguel, Nicolas Casaretto, Albano Cossaro, Luca Floreano, Morten Madsen, and Nadine Witkowski*

ABSTRACT: Organic photovoltaics (OPVs) technology now offers power conversion efficiency (PCE) of over 18% and is one of the main emerging photovoltaic technologies. In such devices, titanium dioxide (TiO_x) has been vastly used as an electron extraction layer, typically showing unwanted charge-extraction barriers and the need for light-soaking. In the present work, using advanced photoemission spectroscopies, we investigate the electronic interplay at the interface between low-temperature-sputtered TiO_x and C_{70} acceptor fullerene molecules. We show that defect states in the band gap of TiO_x are quenched by C_{70} while an interfacial state appears. This new interfacial state is expected to support the favorable energy band alignment observed, showing a perfect match of transport levels, and thus barrier-free extraction of charges, making low-temperature-sputtered TiO_x a good candidate for the next generation of organic solar cells.

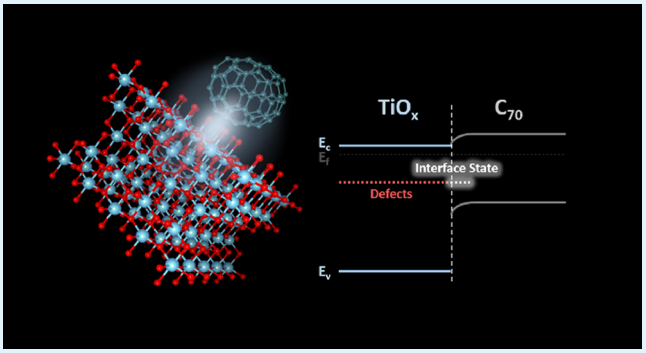

KEYWORDS: *organic solar cell, interface state, titanium dioxide, light-soaking, resonant photoemission, fullerene, gap state*

1. INTRODUCTION

Solar energy is by far the most abundant and widespread renewable energy resource, which is maintenance-free and envisioned to play a key role in the energy transition needed for the next decades. Even though the cost of solar energy has dropped significantly over the past decade, the deployment of large-scale and urban compatible solar installations is still marginal. Organic photovoltaics (OPVs) technology now offers power conversion efficiency (PCE) of over 18%[1] and provides the additional possibility for flexible panels and especially cost-effective printing techniques from roll-to-roll (R2R) processing technology.[2,3] Their lightweight, mechanical flexibility, and semitransparency allow completely new photovoltaic integration schemes, also targeting aesthetic design aspects.[4]

The use of metal oxide interfacial layers acting as hole or electron-transport layer (HTL and ETL, respectively) in organic solar cells has been investigated intensively over the past years, as such layers have a strong impact on both the power conversion efficiency and stability of the devices.[5−7] Titanium oxide (TiO_x) represents such n-type metal oxide extensively used as the electron selective transport layer in both standard and inverted organic solar cells.[8,9]

A feature of some general validity for TiO_x electron-transport layers in organic solar cells is the appearance of s-shape characteristics in the $J-V$ curves of the resulting solar cell devices, arising from an energy-level misalignment, i.e., an electron extraction barrier, at the interface between the TiO_x layer and the organic electron acceptor.[10−12] This s-shape has been demonstrated to disappear as a function of UV light-soaking. The neutralization of the negatively charged chemisorbed oxygen appearing at the TiO_x surface, followed by oxygen desorption,[13,14] results in the restoration of the low work function of the TiO_x thin film upon exposure to UV light, providing a more ideal electron selective contact to the organic electron acceptor molecules.[12]

Recently, we have reported on a low-temperature sputtering process for TiO_x electron-transport layers that allows for efficient electron extraction and thus high power conversion efficiencies without any s-shape formation[15] and thus no need for light activation. The performance is strongly correlated with the formation of crystalline phases in the TiO_x films; however, the effect from local electronic property variations across the surface and at the interface with the organic active layer, which potentially have a strong impact on the electron extraction properties and thus the performance of the related devices, has to date not been investigated.

Accepted: April 8, 2021

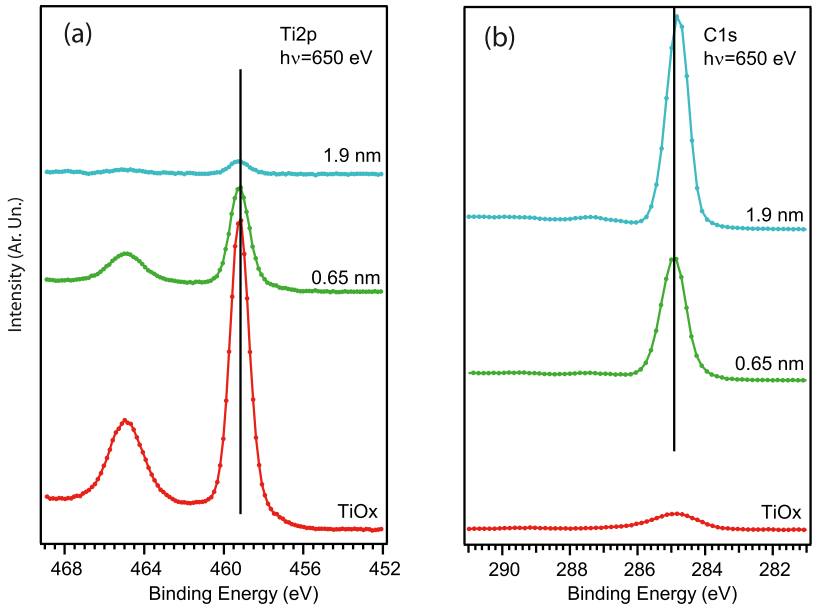

Figure 1. TiO_x sputtered at 150 °C: Ti 2p core-level emission spectra (a) and C 1s core-level emission spectra (b) for the increasing C_{70} thicknesses.

In the present work, we investigate the electronic interface between TiO_x electron-transport layers, formed by sputtering at low temperature, and the prototypical fullerene acceptor molecule C_{70}. By combining photoemission spectroscopies, absorption spectroscopies, and resonant photoemission, we are able to draw a detailed energy band alignment at the interfacial region evidencing a perfect match between the transport levels for electrons, i.e., supporting barrier-free electron extraction. Furthermore, we are able to show the presence of defect states from the TiO_x surface. Those states, located within the band gap of the material, are found to be quenched at the interface with C_{70} molecules while the presence of an interfacial state is evidenced. This could explain the absence of s-shape characteristics in the $J-V$ curves of these sputtered TiO_x-based devices, i.e., also without light-soaking, making them highly relevant for organic solar cell devices.

2. EXPERIMENTAL SECTION

2.1. Experimental Techniques. X-ray photoelectron spectroscopies (XPS, ultraviolet photoelectron spectroscopy (UPS), resonant photoemission (RESPES)) have been carried out at ALOISA beamline from ELETTRA synchrotron facility using hemispherical electron energy analyzer under normal emission with a resolving power of about 5000 with X-ray beam impinging in grazing incidence.

The X-ray absorption spectroscopy (XAS) experiment was performed at $L_{3,2}$ Ti edge in partial electron yield mode by means of a channeltron equipped with a negatively biased grid set to −420 V to filter out low-energy secondary electrons and increase the signal-to-background ratio. The spectra were taken at the so-called "magic angle", with the impinging electric field polarization at about 55° from the surface normal. The overall energy resolution was set to about 100 meV.[16] The intensity was normalized with incoming flux recorded on the premirror and photon energy was scaled relative to the main peak tabulated at 458 eV by Chen et al. on TiO_2 anatase and rutile phase.[17] Resonant photoemission (RESPES) was performed as a series of photoemission spectra across the $L_{2,3}$ Ti in a wide kinetic energy range including both Ti3p and valence states using constant initial state mode. With the second-order light giving satellite feature overlapping the valence band, this peak was subtracted from the on-resonance spectra by fitting the peak shape and intensity at photon energies where the peak appeared well separated from any other valence band feature. Due to this complication, it was not possible to follow all XA resonances.

2.2. Sample Preparation. TiO_x samples prepared in Denmark were deposited on fused silica glass precoated with indium tin oxide (ITO) using radio frequency (RF) sputtering of titanium target (purity of 99.97% from Kurt-lesker) under a base pressure of 10^{-8} mbar. The samples were annealed to 150 °C in ultrahigh vacuum (10^{-8} mbar) prior to the start of the deposition and kept at the set temperature for 30 min during the deposition. To sputter titanium, 10 sccm of argon gas was used to create the plasma, reaching the processing pressure of 3×10^{-3} mbar. Keeping the process pressure constant, a mixture of 8.5 sccm of argon mixed with 1.5 sccm of oxygen was used to form the TiO_x film. The film thickness was monitored using a crystal quartz microbalance. After finishing the sputtering process, the samples were kept in ultrahigh vacuum for 60 min to cool down. Upon cooling, the samples were transferred to a nitrogen-filled glovebox where they were placed in an aluminum-wrapped sample box and vacuum sealed for further characterization at the ELETTRA synchrotron. The samples were annealed to 170 °C prior to the in situ organic molecule deposition to reduce carbon contamination from atmospheric exposure. There was no evidence of any change in titanium oxidation state upon annealing.

Fullerene C_{70} molecules from Sigma-Aldrich were first outgassed at about 250 °C until the base pressure was recovered in the process chamber. The C_{70} evaporations on the TiO_x surface were monitored using a quartz oscillator and thicknesses were evaluated from substrate intensity attenuation as described in ref 18.

3. RESULTS AND DISCUSSION

3.1. Photoemission Results. Figure 1a,b presents the spectra, respectively, recorded on the Ti 2p and C 1s core levels at the photon energy of 650 eV for increasing thicknesses of the C_{70} molecules. The Ti $2p^{3/2}$ core-level binding energy was calibrated relative to the Fermi energy visible on the sample and was found at a binding energy of 459.2 eV, which is very close to the value determined on the TiO_x sample prepared in similar conditions,[15] confirming the Ti^{4+} character of the Ti ions. A fitting procedure of the Ti $2p^{3/2}$ core level, detailed in the Supporting Information (Fig. S1), shows that 78% of the signal is represented by Ti^{4+}, whereas 12% are attributed to the Ti^{3+} states. Note that prior to C_{70} deposition,

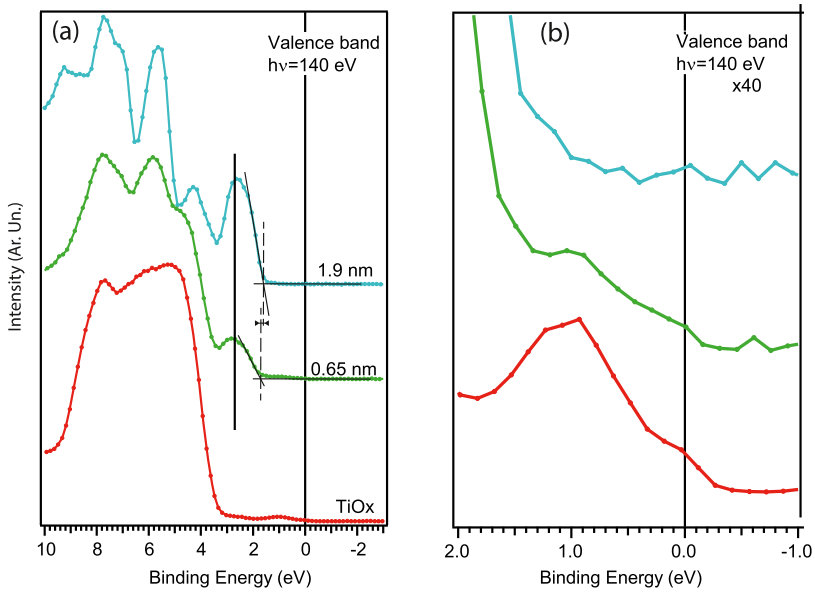

Figure 2. TiO_x sputtered at 150 °C: valence band spectra (a) for increasing thicknesses and valence band onsets located at 1.7 eV (0.65 nm of C_{70}) and 1.6 eV (1.9 nm of C_{70}) below the Fermi level are indicated by dashed lines. (b) Zoom ×40 of the Fermi region.

the TiO_x substrate still displays a C 1s peak characteristic of residual carbon contamination. While increasing the C_{70} thickness on the sputtered TiO_x from 0.65 to 1.9 nm does not affect Ti 2p (Figure 1a and O 1s, not shown here), the C 1s peak associated with C_{70} shows a slight shift toward lower binding energy by 0.1 eV. The C 1s binding energy position is found at 284.83 eV for a film thickness of about 2 nm, which is in line with the spectra measured on the C_{70} thick film.[19] Similar results have been obtained for the TiO_x samples sputtered at 350 °C for which a shift of 0.16 eV is observed for the C 1s orbitals when the C_{70} thicknesses vary from 0.45 to 1.9 nm (see Figure S2 of the Supporting Information).

The valence band presented in Figure 2 shows a pronounced spectral feature at about 1 eV on the pristine sample of TiO_x, which can be attributed to excess electrons created by oxygen vacancies, which partially fill Ti 3d orbitals in the surface and subsurface region.[20] We also observe a small step at the Fermi level, which is even larger on the film sputtered at 350 °C (see Figure S2) and indicates a slight metallic character at the surface of the oxide. Former measurements on the anatase TiO_2(101) surface suggested the occurrence of a shallow gap state at the Fermi level associated with the undercoordinated Ti^{4+} atoms at the step edges;[21] however, this possibility is ruled out on the basis of the resonant photoemission measurements at the Ti 2p ionization threshold, which do not display any resonating behavior at the Fermi position (see next section). The highest occupied molecular orbital (HOMO) level peak of C_{70} is evidenced already for a 0.65 nm thickness by a feature centered around 2.65 eV from the Fermi energy, which encounters an energy shift toward the Fermi energy for a larger thickness of 1.9 nm, which is of the same order of magnitude than the one observed for the C 1s core level, characterizing a band bending at the C_{70}/TiO_x interface. This finding is very similar to what has been observed at the C60/TiO_x interface by Trost et al.[12] Also, as for the Ti 2p core levels, no shift has been evidenced in the Ti 3p valence orbitals at 37.75 eV upon the C_{70} deposition. Looking closely at the Fermi region presented in Figure 2b, a 0.65 nm thick C_{70} film displays a feature at 1 eV, which disappears for thicker films. As shown in the Supporting Information and discussed in the following sections, the intensity of the band gap spectral feature at 0.65 nm is much larger than what is expected from a simple attenuation due to the C_{70} film. It is of utmost importance to get a better chemical insight in the state at 1 eV remaining after C_{70} deposition.

3.2. Absorption and RESPES Results. To better understand the modification of the electronic structure at the C_{70}/TiO_x interface, X-ray absorption spectra at the Ti $L_{3,2}$ edge have been recorded for the pristine TiO_x and with the addition of a thin layer of C_{70}; the results are shown in Figure 3a. The X-ray absorption spectra occur from excitations of a core electron in the 2p level to the unoccupied 3d states, corresponding to a transition from a ground state $2p^6\ 3d^n$ to an excited electronic configuration $2p^5\ 3d^{n+1}$. Because of the spin−orbit degeneracy in the 2p state, the XA spectra contain two dominant features in the energy ranges 455−462 eV and 462−469 eV, which correspond to the $2p^{3/2}$ to 3d transition (L3) and $2p^{1/2}$ to 3d transition (L2), respectively. The main peak at 458 eV is associated with transitions to the final states $2p_{3/2}\ 3d(e_g)$ and the feature at 460 eV to the final states $2p_{3/2}\ 3d(t_{2g})$ split into d_{z^2} and $d_{x^2+y^2}$.[22] The presented XA spectra are very similar to the ones characterizing the anatase phase[17] presenting noncubic structural distortion of the Ti−O tetrahedra as also confirmed by the ex situ XRD measurements recorded after the XA experiments (see Figure S3 of the Supporting Information). Weak differences were observed on the Ti $L_{3,2}$ edge before and after deposition of 0.65 nm of C_{70}, indicating that Ti empty orbitals are only weakly affected by the molecules. Even if slight deviations in XA spectra are observed at the transition associated with the t_{2g} final states, it is difficult to attribute them to the interfacial interplay or resulting from structural inhomogeneities of the samples.

To elaborate on the interplay between the C_{70} and TiO_x interface, RESPES at the Ti 2p edge has been recorded before and after the C_{70} deposition. This technique can be used to gain insights into the ground-state electronic structure of 3d orbitals in titanium dioxides at surfaces and interfaces,[23−25] which is of particular interest for solar cell applications. In this

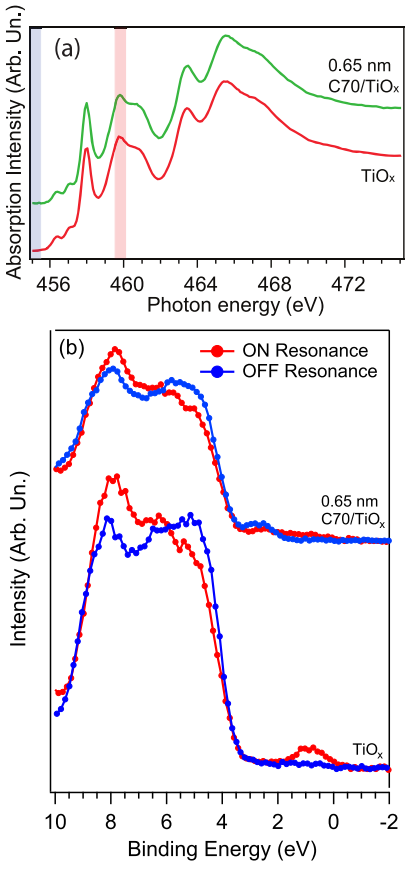

Figure 3. (a) Absorption at Ti $L_{3,2}$-edge (2p-3d). (b) All energy distribution curves on TiO_x and 0.65 nm C_{70}/TiO_x at photon energies corresponding to the on- and off-resonance at photon energies around 455 and 460 eV, as illustrated by colored stripes in the absorption spectra.

technique, interferences may occur for a transition from a ground state to a final state via two channels: either by direct photoemission from valence states or by an indirect channel, where the absorbed photon promotes a core electron from the Ti 2p orbitals to Ti the 3d empty orbitals (either e_g or t_{2g} orbitals depending on the incoming photon energy), which then, by an auto-ionization process (resonant Auger decay), leads to the ejection of an electron from a valence state having the same kinetic energy as a photoelectron emitted from the direct process.[26] In this technique, the incoming photon energy is tuned to resonate with the energy of the Ti 2p to Ti 3d transition, enhancing its photoemission cross section. This makes this technique particularly sensitive to the presence of the 3d states in the band gap. The RESPES spectra are presented in Figure 3b, where off-resonance spectra have been measured for the Ti L3 edge around 455 eV of the incoming photon energy and on-resonance at the transition to $2p_{3/2}$ $3d(t_{2g})$. Because of a second-order satellite feature, it was not possible to extract reliable analysis on other transitions. For the pristine surface of TiO_x, a clear difference in the intensity is observed between on- and off-resonance especially at about 1 eV from the Fermi energy. Even if these states are present in the sample and visible at low photon energies, their photoemission cross section is very weak when the photon energy is tuned to 455 eV. However, when the photon energy is tuned to the Ti 2p to $3d(t_{2g})$ absorption, the cross section is enhanced and the feature appears, making this technique particularly sensitive to defect states at the TiO_x interfaces. The same experiment has been repeated at the interface between C_{70} and TiO_x resulting in very different observations. A new feature is observed at 2.65 eV for both on- and off-resonance spectra. This state corresponds to the C_{70} HOMO, as previously observed at a photon energy of 140 eV, even if its intensity at a $h\nu$ = 455−460 eV is much smaller, due to the decrease of cross section at the Ti 2p ionization threshold.

After the adsorption of C_{70} molecules, Ti 3d states present in the band gap are quenched as shown by RESPES, whereas a state lying at about 1 eV below the Fermi level is evidenced only at low photon energy in the gap, suggesting that the observed Ti 3d states are modified when in contact with the C_{70} molecules. We conclude from these observations that the nature of the gap states might change for the pristine TiO_x and at the interface with the C_{70} molecules. This result will be further discussed in the next section.

3.3. Discussion. Based on the experiments carried out, we can draw a detailed band diagram at the interface as represented in Figure 4. The positions of the valence band

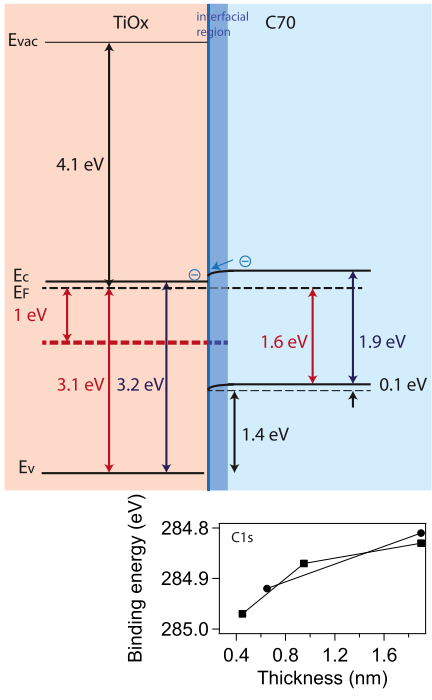

Figure 4. Top: band diagrams of C $70/TiO_x$ as derived from the photoemission spectra. Energy gaps are extracted according to optical absorption data.[15,27] Bottom: variation of the binding energy of C 1s versus C_{70} thickness for TiO_x sputtered at 150 °C (circle) and TiO_x sputtered at 350 °C (square).

onset energy have been extracted from experimental data presented in Figure 2. The conduction band positions have been determined from the optical absorption gap of 3.2 eV for TiO_x[15] and 1.9 eV for C_{70}.[27] The TiO_x work function has been measured on a sample prepared in similar conditions,[15] as it was not possible to measure the work function at the C_{70}/TiO_x interface in situ at the ALOISA beamline. Photoemission on both core level and valence band has evidenced a downward band bending of about 0.1 eV from the C_{70} electronic levels toward the TiO_x electronic levels, which may favor the electron transfer from the C_{70} to the TiO_x layer. The measured band bending is probably underestimated as it results from the

energy difference between 1.9 nm of C_{70}, which can be considered as bulk value for photoemission, and 0.65 nm of C_{70}, which is probably not pure interfacial contribution due to surface inhomogeneities. Larger band bending is indeed measured on a sample sputtered at 350 °C for thinner deposition (see the Supporting Information). Despite the above limitation, the present finding is different than the results obtained for different TiO_x films (nonsputtered) by Trost et al.,[12] in which the typical energy barrier between the lowest unoccupied molecular orbital (LUMO) level of C60 fullerene and the conduction band of TiO_x is evidenced, on a titanium oxide film showing typical s-shape behavior. Our presented results could thus explain the reason for the lack of s-shape characteristics recently observed in organic solar cell devices that are based on similar sputtered TiO_x layers,[15] as no electron extraction barrier between the C_{70} LUMO and the TiO_x conduction band is present for these sputtered TiO_x films. The lack of an extraction barrier supports efficient electron extraction across the C_{70}/TiO_x interface, leading to the well-performing TiO_x-based organic solar cell devices without the need for UV light-soaking.[15]

In our system, the RESPES experiment shows that Ti defect states are quenched at the C_{70} interface. On the other hand, a weak feature is still visible at about 1 eV in the valence band, when the photon energy is tuned to 140 eV (see Figure 2b), which could be attributed to the formation of an interfacial state with C_{70}. Our conclusions are consistent with the quantitative analysis of the valence band, as measured at 140 eV and presented in the following. The interface layer of C_{70} was first estimated to be 0.65 nm using the intensity attenuation of the core-level state of the substrate. Considering the size of C_{70} molecules, it can be estimated that only 10% of the TiO_x surface is not covered by C_{70} molecules. The observed 3d "defect states" at 1 eV in the valence band should correspond to 10% of TiO_x uncovered surface and 90% buried interface. However, using valence band data, estimations show that the signal obtained is twice as large as expected. This first indicates that the signal at 1 eV in the binding energy at the interface does not only arise from Ti-related defect states buried under the C_{70} layer but that some states in the C_{70} layer located at the same binding energy must also participate in the signal. This observation is then reinforced by the absence of signal in the RESPES spectra of the interface, which confirms that the state is no longer due to the Ti 3d defect states when it comes to the interface with the C_{70} layer. This information altogether seems to point toward the formation of a new state at the interface between C_{70} and TiO_x, involving Ti 3d states from the TiO_x surface. All details on estimations are given in the Supporting Information. Such interfacial behavior has already been reported for similar systems such as ZnO/C_{60},[28] $PTCDI/TiO_2$,[29] and Ru(II)-dye/TiO_2.[30] In both these systems, it is demonstrated that Ti defect state at the metal oxide surface are borne by a new state at the interface with organic molecules. In both cases, the defect state at the surface metal oxide surface before deposition and the new interfacial state is found to lie at approximately the same binding energy, which is also the case for our system.

As noted above, the presented energy diagram can explain the lack of s-shape characteristics measured in solar cells recently prepared with similar TiO_x layers sputtered at 150 °C.[15] Indeed, the presence of oxygen vacancies induces extra electrons acting as shallow donor-like states that create an accumulation layer in the near-surface region.[20,31] After the adsorption of C_{70} molecules, Ti 3d states are quenched and an interfacial state lying at about 1 eV below the Fermi level is evidenced. The exact role of the interfacial state on the charge transport across the interface taking place in organic solar cell devices, however, remains unclear. Notably, the location at about 1 eV below the TiO_x conduction band minimum does not make it well suited for direct charge extraction. However, the interfacial state could well play an important role in the favorable energy band lineup presented and also (or related) on the unwanted sensitivity of the TiO_x surface to oxygen adsorption/desorption processes typically observed for other TiO_x layers in organic solar cells.

4. CONCLUSIONS

In summary, our study proposes a thorough electronic investigation of the interface of fullerene with low-temperature-sputtered TiO_x. Using the chemical selectivity offered by the resonant photoemission at the Ti $L_{3,2}$ edge, we evidence the quenching of defect gap state in TiO_x along with fullerene deposition with the persistence of gap state, whose chemical nature is different from that of pristine TiO_x. The resulting energy band alignment obtained by combining valence band and core-level photoemission shows barrier-free charge-extraction properties and thus demonstrates that the sputtered TiO_x layers are good candidates as electron extraction layers at the interface with fullerene acceptors in organic solar cells without the need for UV light-soaking.

■ ASSOCIATED CONTENT

Deconvolution of Ti 2p emission spectra (presented here as Figure 1a), XPS measurements performed on TiO_x sample sputtered at 350 °C, and XRD measurements on both TiO_x samples sputtered at 150 and 350 °C. It also contains details on the coverage estimations of the C_{70}/TiO_x interface presented here and fitted defect states in the valence band spectra for both pristine TiO_x surface and interface (PDF)

■ AUTHOR INFORMATION

Corresponding Author

Nadine Witkowski − *Sorbonne Université, UMR CNRS 7588, Institut des Nanosciences de Paris, F-75005 Paris, France;* orcid.org/0000-0002-7583-1218; Email: nadine.witkowski@sorbonne-universite.fr

Authors

Dylan Amelot − *Sorbonne Université, UMR CNRS 7588, Institut des Nanosciences de Paris, F-75005 Paris, France;* orcid.org/0000-0001-9908-810X

Mehrad Ahmadpour − *SDU NanoSYD, Mads Clausen Institute, University of Southern Denmark, Sønderborg DK-6400, Denmark;* orcid.org/0000-0001-9722-4163

Quim Ros − *Sorbonne Université, UMR CNRS 7588, Institut des Nanosciences de Paris, F-75005 Paris, France*

Hervé Cruguel − *Sorbonne Université, UMR CNRS 7588, Institut des Nanosciences de Paris, F-75005 Paris, France*

Nicolas Casaretto − *Sorbonne Université, UMR CNRS 7588, Institut des Nanosciences de Paris, F-75005 Paris, France*

Albano Cossaro − *Department of Chemical and Pharmaceutical Sciences, University of Trieste, Trieste 34127, Italy; CNR-IOM, Trieste 34149, Italy;* orcid.org/0000-0002-8429-1727

Luca Floreano − *CNR-IOM, Trieste 34149, Italy;* orcid.org/0000-0002-3654-3408

Morten Madsen − *SDU NanoSYD, Mads Clausen Institute, University of Southern Denmark, Sønderborg DK-6400, Denmark;* orcid.org/0000-0001-6503-0479

Complete contact information is available at: https://pubs.acs.org/10.1021/acsami.1c01966

Notes

The authors declare no competing financial interest.

■ ACKNOWLEDGMENTS

We are grateful to ALOISA beamline staff for providing support and assistance during the beamtime. We acknowledge the financial support from ALOISA synchrotron facility. M.M. acknowledges Danmarks Frie Forskningsfond, DFF FTP for funding of the project React-PV, No. 8022-00389B and the support from the project SMART—Structure of MAterials in Real Time, funded by the Danish Ministry of Higher Education and Science. The research leading to this result has been supported by the project CALIPSOplus under the Grant Agreement 730872 from the EU Framework Program for Research and Innovation HORIZON 2020.

■ REFERENCES

(1) Liu, Q.; Jiang, Y.; Jin, K.; Qin, J.; Xu, J.; Li, W.; Xiong, J.; Liu, J.; Xiao, Z.; Sun, K.; Yang, S.; Zhang, X.; Ding, L. 18% Efficiency Organic Solar Cells. *Sci. Bull.* **2020**, *65*, 272−275.

(2) Lucera, L.; Machui, F.; Kubis, P.; Schmidt, H. D.; Adams, J.; Strohm, S.; Ahmad, T.; Forberich, K.; Egelhaaf, H.-J.; Brabec, C. J. Highly Efficient, Large Area, Roll Coated Flexible and Rigid OPV Modules with Geometric Fill Factors Up to 98.5% Processed with Commercially Available Materials. *Energy Environ. Sci.* **2016**, *9*, 89−94.

(3) Destouesse, E.; Top, M.; Lamminaho, J.; Rubahn, H.-G.; Fahlteich, J.; Madsen, M. Slot-Die Processing and Encapsulation of Non-Fullerene Based ITO-Free Organic Solar Cells and Modules. *Flexible Printed Electron.* **2019**, *4*, No. 045004.

(4) Berny, S.; et al. Solar Trees: First Large-Scale Demonstration of Fully Solution Coated, Semitransparent, Flexible Organic Photovoltaic Modules. *Adv. Sci* **2016**, *3*, No. 1500342.

(5) Ahmadpour, M.; Fernandes Cauduro, A. L.; Méthivier, C.; Kunert, B.; Labanti, R.; Resel, C.; Turkovic, V.; Rubahn, H.; Witkowski, N.; Schmid, A. K.; Madsen, M. Crystalline Molybdenum Oxide Layers as Efficient and Stable Hole Contacts in Organic Photovoltaic Devices. *ACS Appl. Energy Mater.* **2019**, *2*, 420−427.

(6) Greiner, M. T.; Helander, M. G.; Tang, W.-M.; Wang, Z.-b.; Qiu, J.; Lu, Z.-h. Universal Energy-Level Alignment of Molecules on Metal Oxides. *Nat. Mater.* **2012**, *11*, 76−81.

(7) Olthof, S.; Riedl, T. Chapter 3: Metal-Oxide Interface Materials for Organic and Perovskite Solar Cells. *Wolrd Sci. Ref. Hybrid Mater.* **2019**, *2*, 61−104.

(8) Park, S. H.; Roy, A.; Beaupré, S.; Cho, S.; Coates, N.; Moon, J. S.; Moses, D.; Leclerc, M.; Lee, K.; Heeger, A. J. Bulk Heterojunction Solar Cells with Internal Quantum Efficiency Approaching 100%. *Nat. Photonics* **2009**, *3*, 297−302.

(9) Waldauf, C.; Morana, M.; Denk, P.; Schilinsky, P.; Coakley, K.; Choulis, S. A.; Brabec, C. J. Highly Efficient Inverted Organic Photovoltaics Using Solution Based Titanium Oxide as Electron Selective Contact. *Appl. Phys. Lett.* **2006**, *89*, No. 233517.

(10) Kim, J.; Kim, G.; Choi, Y.; Lee, J.; Heum Park, S.; Lee, K. Light-Soaking Issue in Polymer Solar Cells: Photoinduced Energy Level Alignment at the Sol-Gel Processed Metal Oxide and Indium Tin Oxide Interface. *J. Appl. Phys.* **2012**, *111*, No. 114511.

(11) Lin, Z.; Jiang, C.; Zhu, C.; Zhang, J. Development of Inverted Organic Solar Cells with TiO2 Interface Layer by Using Low-Temperature Atomic Layer Deposition. *ACS Appl. Mater. Interfaces* **2013**, *5*, 713−718.

(12) Trost, S.; Zilberberg, K.; Behrendt, A.; Polywka, A.; Görrn, P.; Reckers, P.; Maibach, J.; Mayer, T.; Riedl, T. Overcoming the "Light-Soaking" Issue in Inverted Organic Solar Cells by the Use of Al:ZnO Electron Extraction Layers. *Adv. Energy Mater.* **2013**, *3*, 1437−1444.

(13) Schmidt, H.; Zilberberg, K.; Schmale, S.; Flügge, H.; Riedl, T.; Kowalsky, W. Transient Characteristics of Inverted Polymer Solar Cells Using Titanium Oxide Interlayers. *Appl. Phys. Lett.* **2010**, *96*, No. 243305.

(14) Wilken, S.; Parisi, J.; Borchert, H. Role of Oxygen Adsorption in Nanocrystalline ZnO Interfacial Layers for Polymer-Fullerene Bulk Heterojunction Solar Cells. *J. Phys. Chem. C* **2014**, *118*, 19672−19682.

(15) Mirsafaei, M.; Jensen, P. B.; Ahmadpour, M.; Lakhotiya, H.; Hansen, J. L.; Julsgaard, B.; Rubahn, H.-G.; Lazzari, R.; Witkowski, N.; Balling, P.; Madsen, M. Sputter-Deposited Titanium Oxide Layers as Efficient Electron Selective Contacts in Organic Photovoltaic Devices. *ACS Appl. Energy Mater.* **2020**, *3*, 253−259.

(16) Floreano, L.; Naletto, G.; Cvetko, D.; Gotter, R.; Malvezzi, M.; Marassi, L.; Morgante, A.; Santaniello, A.; Verdini, A.; Tommasini, F.; Tondello, G. Performance of the Grating-Crystal Monochromator of the ALOISA Beamline at the Elettra Synchrotron. *Rev. Sci. Instrum.* **1999**, *70*, 3855−3864.

(17) Chen, C. L.; Dong, C.-L.; Chen, C.-H.; Wu, J.-W.; Lu, Y.-R.; Lin, C.-J.; Ya Hsuan Liou, S.; Tseng, C.-M.; Kumar, K.; Wei, D.-H.; Guo, J.; Chou, W.-C.; Wu, M.-K. Electronic Properties of Free-Standing TiO2 Nanotube Arrays Fabricated by Electrochemical Anodization. *Phys. Chem. Chem. Phys.* **2015**, *17*, 22064−22071.

(18) Hufner, S. *Photoelectron Spectroscopy: Principles and Applications*, 2nd ed.; Springer-Verlag, 1996.

(19) Han, B.-y.; Yu, L.-m.; Hevesi, K.; Gensterblum, G.; Rudolf, P.; Pireaux, J.-J.; Thiry, P. A.; Caudano, R.; Lambin, P.; Lucas, A. A. Electronic Transitions and Excitations in Solid C_{70} Studied by EELS and XPS C 1s Satellite Structures. *Phys. Rev. B* **1995**, *51*, 7179−7185.

(20) Kruger, P.; Bourgeois, S.; Domenichini, B.; Magnan, H.; Chandesris, D.; Le Fevre, P.; Flank, A. M.; Jupille, J.; Floreano, L.; Cossaro, A.; Verdini, A.; Morgante, A. Defect States at the TiO2(110) Surface Probed by Resonant Photoelectron Diffraction. *Phys. Rev. Lett.* **2008**, *100*, No. 055501.

(21) Reckers, P.; Dimamay, M.; Klett, J.; Trost, S.; Zilberberg, K.; Riedl, T.; Parkinson, B. A.; Brötz, J.; Jaegermann, W.; Mayer, T. Deep and Shallow TiO_2 Gap States on Cleaved Anatase Single Crystal (101) Surfaces, Nanocrystalline Anatase Films, and ALD Titania Ante and Post Annealing. *J. Phys. Chem. C* **2015**, *119*, 9890−9898.

(22) Diebold, U. The Surface Science of Titanium Dioxide. *Surf. Sci. Rep.* **2003**, *48*, 53−229.

(23) Okada, K.; Kotani, A. Theory of Core Level X-Ray Photoemission and Photoabsorption in Ti Compounds. *J. Electron Spectrosc. Relat. Phenom.* **1993**, *62*, 131−140.

(24) Prince, K. C.; Dhanak, V. R.; Finetti, P.; Walsh, J. F.; Davis, R.; Muryn, C. A.; Dhariwal, H. S.; Thornton, G.; van der Laan, G. 2p Resonant Photoemission Study of TiO_2s. *Phys. Rev. B* **1997**, *55*, 9520−9523.

(25) Sánchez-Agudo, M.; Soriano, L.; Quirós, C.; Abbate, M.; Roca, L.; Avila, J.; Sanz, J. M. Resonant Photoemission and X-ray Absorption Study of the Electronic Structure of the TiO_2-Al_2O_3 Interface. *Langmuir* **2001**, *17*, 7339−7343.

(26) De Groot, F.; Kotani, A. *Core Level Spectroscopy of Solids*, Advances in Condensed Matter Science; Taylor & Francis Group, 2008.

(27) Sherafatipour, G.; Benduhn, J.; Patil, B. R.; Ahmadpour, M.; Spoltore, D.; Rubahn, H.-G.; Vandewal, K.; Madsen, M. Degradation Pathways in Standard and Inverted DBP-C-70 Based Organic Solar Cells. *Sci. Rep.* **2019**, *9*, No. 4024.

(28) Schulz, P.; Kelly, L. L.; Winget, P.; Li, H.; Kim, H.; Ndione, P. F.; Sigdel, A. K.; Berry, J. J.; Graham, S.; Brédas, J.-L.; Kahn, A.; Monti, O. L. A. Tailoring Electron-Transfer Barriers for Zinc Oxide/C60 Fullerene Interfaces. *Adv. Funct. Mater.* **2014**, *24*, 7381−7389.
(29) Lanzilotto, V.; Lovat, G.; Fratesi, G.; Bavdek, G.; Brivio, G. P.; Floreano, L. TiO(110) Charge Donation to an Extented π -Conjugated Molecule. *J. Phys. Chem. Lett.* **2015**, *6*, 308−313.
(30) Schwanitz, K.; Weiler, U.; Hunger, R.; Mayer, T.; Jaegermann, W. Synchrtron-Induced Photoelectron Spectroscopy of the Dye-Sensitized Nanocrystalline TiO_2/Electrolyte Interface: Band Gap States and Their Interaction with Dye and Solvent Molecules. *J. Phys. Chem. C* **2007**, *111*, 849−854.
(31) Moses, P. G.; Janotti, A.; Franchini, C.; Kresse, G.; Van de Walle, C. G. Donor Defects and Small Polarons on the TiO_2(110) Surface. *J. Appl. Phys.* **2016**, *119*, No. 181503.